

## On the total number of distinct self-interacting self-avoiding walks on three-dimensional fractal structures

This article has been downloaded from IOPscience. Please scroll down to see the full text article.

2005 J. Phys. A: Math. Gen. 38 555

(<http://iopscience.iop.org/0305-4470/38/3/003>)

View [the table of contents for this issue](#), or go to the [journal homepage](#) for more

Download details:

IP Address: 171.66.16.92

The article was downloaded on 03/06/2010 at 03:51

Please note that [terms and conditions apply](#).

# On the total number of distinct self-interacting self-avoiding walks on three-dimensional fractal structures

I Živić<sup>1</sup>, S Milošević<sup>2</sup> and B Djordjević<sup>1</sup>

<sup>1</sup> Faculty of Natural Sciences and Mathematics, University of Kragujevac, 34000 Kragujevac, Serbia

<sup>2</sup> Faculty of Physics, University of Belgrade, PO Box 368, 11001 Belgrade, Serbia

E-mail: ivanz@kg.ac.yu and emilosev@etf.bg.ac.yu

Received 16 July 2004, in final form 8 November 2004

Published 23 December 2004

Online at [stacks.iop.org/JPhysA/38/555](http://stacks.iop.org/JPhysA/38/555)

## Abstract

We have studied self-interacting self-avoiding walks (SAWs) situated on three-dimensional fractal structures, represented by a 3D Sierpinski gasket (SG) family of fractals. To this end, we have applied the exact renormalization group method (for the first three members of the SG fractal family,  $b = 2, 3$  and 4) to calculate the critical exponents  $\gamma_E$ ,  $\gamma_\theta$  and  $\gamma_G$  (associated with the total number of distinct SAWs in extended phase,  $\theta$ -chain and globular-collapsed polymer phase, respectively). To extend the obtained sequence of exact values for  $\gamma_E$ , we have applied the Monte Carlo renormalization group method for fractals with  $2 \leq b \leq 40$ . Our results demonstrate that the critical exponent  $\gamma_E$ , as a function of  $b$ , monotonically increases and is always larger than the corresponding three-dimensional Euclidean value. On the other hand,  $\gamma_\theta$  (for the values  $b = 2, 3$  and 4), being smaller than the corresponding Euclidean value, decreases with  $b$ .

PACS numbers: 64.60.Ak, 36.20.Ey, 05.40.Fb, 05.50.+q

## 1. Introduction

The self-avoiding walk (SAW) is a random walk whose path must not contain self-intersections. This kind of random walk may serve as a model of a linear polymer. For the model situated on a lattice, it is assumed that each visited site represents a monomer. Here we take that two non-consecutive adjacent monomers, along the polymer chain, interact via a short-range interaction. Presence of such interactions causes the so-called  $\theta$  transition from the extended chain polymer phase, that exists at high temperatures, to a globule (collapsed) phase polymer, that appears at low temperatures. The point at which the transition between the two phases

occurs is referred to as the  $\theta$ -point, and the temperature associated with this point is denoted as  $T_\theta$ . The crossover in a chain comprising  $N$  units, from high temperature to low temperature phases, that happens at the  $\theta$ -point, is described by the crossover critical exponent  $\phi_\theta$ , which determines the average number  $\langle M \rangle$  of monomers being in contact,  $\langle M \rangle \sim N^{\phi_\theta}$ . Besides finding the correct value of  $\phi_\theta$ , the main research question concerns the values of the critical exponents  $\nu$  and  $\gamma$  in three different regions (in the extended phase, at the  $\theta$ -point and in the collapsed phase). The critical exponent  $\nu$  is associated with the mean-squared end-to-end distance  $\langle R_N^2 \rangle \sim N^{2\nu}$  of the  $N$ -step SAWs, whereas the critical exponent  $\gamma$  determines the total number of different polymer configurations according to the law  $C_N \sim \mu^N N^{\gamma-1}$ . The critical properties of described self-interacting polymers have been mostly studied for models situated on two-dimensional (2D) and three-dimensional (3D) Euclidean lattices (for a review see, for instance, [1]). In these studies, various theoretical methods were applied, such as the field theoretical approach [2], exact enumeration method [3] and different types of Monte Carlo simulations [4–7].

The above problem has also been studied on fractal lattices. But, in the case of fractals it may be noted that the 2D fractal lattices (embedded in the 2D Euclidean spaces) have been more frequently investigated than the corresponding model in the case of the 3D fractals. Since the 3D fractals definitely may serve as a better description of real systems (porous media, for instance), it is desirable to approach the described model in a case of a set of the 3D fractals.

The first study of the problem for a 3D fractal was done by Dhar [8, 9], who applied the renormalization group (RG) technique in the case of the 3D Sierpinski gasket (SG), with the scale parameter  $b = 2$ . Following the work of Dhar, the study was extended for the same fractal but with  $b = 3$  [10] and  $b = 4$  [11]. Recently, using the exact and the Monte Carlo renormalization group (MCRG) method (specifically for investigating the polymer adsorption problem on a family of 3D SG fractals), the study of the sequence of the SG fractals has been extended up to  $b = 40$  [12]. However, in all these studies, the critical exponent  $\nu$  was calculated, whereas the critical exponent  $\gamma$  has been determined only in a case of non-interacting SAWs for the  $b = 2$  3D SG fractal and in the case of SAWs on truncated  $n$ -simplex lattices (for  $n = 5$  and 6) [13]. Taking a more comprehensive approach to the problem, we perform here an exact and MCRG study of interacting SAWs situated on the members of the 3D SG family of fractals. Thus, we report in this paper results of our exact RG calculation of critical exponents  $\gamma$  and  $\phi_\theta$  for the 3D SG fractals with  $b = 2, 3$  and 4 for the three different temperature regions, together with our findings of  $\gamma$  for a long sequence of fractals with  $2 \leq b \leq 40$  in a high temperature region.

This paper is organized as follows. In section 2, we first describe the 3D SG fractals for general  $b$ . Then, we present the framework of the RG method for studying the statistics of interacting self-avoiding walks, which, as a model of a polymer, display definite interactions between non-contiguous monomers, in a way that should make the method applicable in the case of exact calculations, as well as in the case of the Monte Carlo calculations. Accordingly, in the same section, we explain details of the exact and MCRG calculations of the critical exponents  $\gamma$  and  $\phi_\theta$ , for arbitrary  $b$ . In section 3, we present the obtained exact values of  $\gamma$  and  $\phi_\theta$ , for  $b = 2, 3$  and  $b = 4$ , as well as the sequence of the specific MCRG values of  $\gamma$ , obtained up to  $b = 40$ . Summary of the obtained results and the relevant conclusions are given in section 4.

## 2. Renormalization group scheme

Each member of the 3D SG family of fractals is labelled by the scale parameter  $b = 2, 3, 4, \dots$  and can be constructed recursively starting with the pertinent generator which is a tetrahedron

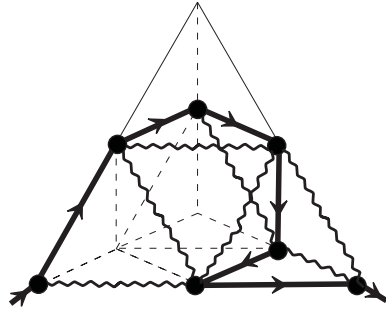


**Figure 1.** The fractal structure of the three-dimensional  $b = 2$  SG fractal at the first stage of construction, with an example of a piece of a possible SAW path (connected solid black segments). The Boltzmann factor  $v = e^{-\epsilon_v/k_B T}$  corresponds to the energy of interaction  $\epsilon_v < 0$  between two non-consecutive neighbouring monomers (depicted by wiggled lines). Thus, for example, the presented SAW configuration should contribute the weight  $x^6 v^7$  in the corresponding RG equation (more specifically, in equation (2.2) for  $r = 0$ ).

of base  $b$  that contains  $b(b+1)(b+2)/6$  unit tetrahedrons. The subsequent fractal stages are constructed self-similarly, by replacing each unit tetrahedron of the initial generator by a new generator. Thus, to obtain the  $r$ th-stage fractal lattice, which we shall call the  $r$ th-order generator, the recursive process has to be repeated  $(r-1)$  times, so that the complete fractal is obtained in the limit  $r \rightarrow \infty$  (see, for instance, figure 1 of [12]). The fractal dimension  $d_f$  of 3D SG fractal is equal to

$$d_f^{3D} = \ln[(b+2)(b+1)b/6]/\ln b. \quad (2.1)$$

It should be observed that the fractal dimension acquires the Euclidean value 3, in the limit  $b \rightarrow \infty$ .

In order to describe the effect of monomer–monomer interaction, we introduce the Boltzmann factor  $v = e^{-\epsilon_v/k_B T}$ , where  $\epsilon_v$  is the energy corresponding to interaction between two non-consecutive neighbouring monomers. If we assign the weight  $x$  to a single step of the SAW walker, then the weight of a walk having  $N$  steps, with  $M$  nearest-neighbour contacts, is  $x^N v^M$  (see figure 1). An arbitrary SAW configuration can be described by using the six restricted generating functions (see figure 2). Due to the self-similarity of the underlying structure, these generating functions appear to be parameters in the corresponding recursion (renormalization group) equations, which (for any  $b \geq 2$ ) have the form

$$A^{(r+1)} = \sum_{i,j} a(i,j) A^i B^j, \quad (2.2)$$

$$B^{(r+1)} = \sum_{i,j} b(i,j) A^i B^j, \quad (2.3)$$

$$C^{(r+1)} = c_1(A,B)C + c_2(A,B)D, \quad (2.4)$$

$$D^{(r+1)} = d_1(A,B)C + d_2(A,B)D, \quad (2.5)$$

$$E^{(r+1)} = e_1(A,B)C^2 + e_2(A,B)D^2 + e_3(A,B)CD + e_4(A,B)E + e_5(A,B)F, \quad (2.6)$$

$$F^{(r+1)} = f_1(A,B)C^2 + f_2(A,B)D^2 + f_3(A,B)CD + f_4(A,B)E + f_5(A,B)F, \quad (2.7)$$

where we have omitted the superscript  $(r)$  on the right-hand side of the above relations. Here, the self-similarity of the underlying fractals implies that numbers  $a(i,j), b(i,j),$

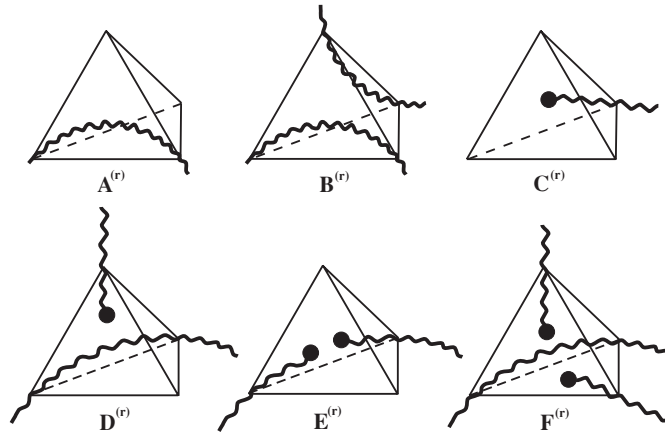


**Figure 2.** Schematic representation of the six restricted generating functions used in describing all possible polymer configurations within the  $r$ th stage 3D SG fractal structure. Thus, for example,  $C^{(r)}$  represents the SAW paths that start somewhere within the  $r$ th-stage fractal structure and leaves it at one tetrahedron vertex. The interior details of the  $r$ th-order fractal structure are not shown (they are manifested by the wiggles of the SAW paths).

and coefficients  $c_1(A, B)$ ,  $c_2(A, B)$ ,  $d_1(A, B)$ ,  $d_2(A, B)$ ,  $e_i(A, B)$  and  $f_i(A, B)$  ( $i = 1, 2, 3, 4, 5$ ), being polynomials in terms of  $A$  and  $B$ , do not depend on  $r$ .

The assumed physical picture of the problem under study suggests that the established RG transformations should be supplemented by the following initial conditions:

$$\begin{aligned} A^{(0)}(x, v) &= x + 2x^2v + 2x^3v^3, & B^{(0)}(x, v) &= x^2v^4, \\ C^{(0)} &= D^{(0)} = E^{(0)} = F^{(0)} = 0, \end{aligned} \quad (2.8)$$

which are pertinent to the elementary tetrahedron ( $r = 0$ ).

We begin analysis of the above set of RG equations by observing that first two equations, (2.2) and (2.3), can be iterated independently from the rest [12]. In short, for small values of the monomer–monomer interaction ( $v < v_\theta$ ), that is, at high temperatures ( $T > T_\theta$ ), the extended SAW phase fixed point

$$(A^*, B^*) = (A_E, B_E), \quad (2.9)$$

is reached by iterating the RG transformations. Linearization of the RG equations (2.2) and (2.3) in the vicinity of this fixed point gives only one relevant eigenvalue  $\lambda_v^E$ , associated with the mean-squared end-to-end distance  $\langle R_N^2 \rangle$  of the  $N$ -step polymer chain. In the general case  $\langle R_N^2 \rangle$  behaves asymptotically (for large  $N$ ) as according to the power law  $\langle R_N^2 \rangle \sim N^{2\nu}$ . Within the RG approach the critical exponent  $\nu$  should be calculated using the formula

$$\nu = \frac{\ln b}{\ln \lambda_v^E}, \quad (2.10)$$

so that, by inserting here  $\lambda_v^E$  we obtain the critical exponent  $\nu_E = \ln b / \ln \lambda_v^E$ , valid at high temperatures  $T > T_\theta$ .

Starting with  $x = x_\theta$  and  $v = v_\theta$  (at  $T = T_\theta$ ), iteration of the RG equations (2.2) and (2.3) leads to the tricritical fixed point

$$(A^*, B^*) = (A_\theta, B_\theta). \quad (2.11)$$

Linearization of (2.2) and (2.3), in the vicinity of this fixed point, produces two relevant eigenvalues  $\lambda_v^\theta$  and  $\lambda_\phi^\theta$  ( $\lambda_v^\theta > \lambda_\phi^\theta$ ). The first gives the critical exponent  $\nu_\theta = \ln b / \ln \lambda_v^\theta$ , which

is smaller than  $v_E$  and which corresponds to the so-called collapse transition. On the other hand, the second eigenvalue  $\lambda_\phi^\theta$  determines the crossover critical exponent

$$\phi_\theta = \frac{\ln \lambda_\phi^\theta}{\ln \lambda_v^\theta}, \tag{2.12}$$

which describes the tricritical scaling  $(x_c - x_\theta) \sim (v - v_\theta)^{1/\phi_\theta}$  of the critical line  $x_c(v)$  in the interaction parameter  $(x, v)$  space.

The physical meaning of the critical exponent  $\phi_\theta$  can be conceived in the following way. The singular part of the internal energy (per monomer) of a polymer system behaves as  $U_N \sim N^{(\alpha-1)\phi_\theta}$ , where  $\alpha$  is the thermal critical exponent [14]. It was proved [15] that, at the collapse transition, critical exponents  $\alpha$  and  $\phi_\theta$  obey the tricritical scaling relation  $2-\alpha = 1/\phi_\theta$ , so that  $U_N \sim N^{\phi_\theta-1}$ . On the other hand, because to each contact between monomers there corresponds the energy  $\varepsilon_v$ , the quantity  $U_N$  can be expressed as  $U_N = \varepsilon_v \langle M \rangle / N$ , where  $\langle M \rangle$  is the average number of monomers in contact. From here it follows that:

$$\langle M \rangle \sim N^{\phi_\theta}, \tag{2.13}$$

which means that the crossover exponent  $\phi_\theta$  determines (at the  $\theta$ -point,  $T = T_\theta$ ) the mean number of monomers in contact.

Depending on the value of the one-step weight (fugacity)  $x$ , for strong monomer–monomer interactions ( $v > v_\theta$ ) RG equations (2.2) and (2.3) bring about the trivial fixed point  $(A, B)^* = (0, 0)$ , for  $x < x_c(v)$ , or  $(A, B)^* = (\infty, \infty)$  for  $x > x_c(v)$ , whereas for  $x$  being precisely equal to  $x_c(v)$ , the corresponding fixed point

$$(A^*, B^*) = (A_G, B_G), \tag{2.14}$$

describes the collapsed globule regime of the polymer system under study. Finally, analysing the RG equations in the vicinity of  $(A_G, B_G)$ , one can find the critical exponent  $\nu_G = \ln b / \ln \lambda_v^G$  which satisfies the relation  $\nu_G < \nu_\theta < \nu_E$ .

In order to find the asymptotic behaviour of the total number  $C(N, T)$  of  $N$ -step SAWs, which is expected, for large  $N$ , to display the following power law:

$$C(N, T) \sim \mu^N N^{\gamma-1} \tag{2.15}$$

with the associated critical exponent  $\gamma$  (and  $\mu$  being the critical connectivity constant) it is necessary to construct the generating function

$$G(x, T) = \sum_{N=1}^{\infty} \sum_{M=1}^N C(N, M) x^N (v(T))^M. \tag{2.16}$$

Here  $C(N, M)$  is the number of  $N$ -step SAWs with  $M$  nearest-neighbour contacts of non-consecutive monomers. Accordingly, we expect the following singular behaviour of the above generating function:

$$G_{\text{sing}} \sim (x_c - x)^{-\gamma}, \tag{2.17}$$

at the critical fugacity  $x_c = x_c(T)$ .

We have verified that, for arbitrary  $b$ , the generating function  $G(x, T)$  is of the form

$$G(x, T) = \sum_{r=0}^{\infty} \left( \frac{6}{b(b+1)(b+2)} \right)^{r+1} \{ p_{CC}(C^{(r)})^2 + p_{CD}C^{(r)}D^{(r)} + p_{DD}(D^{(r)})^2 + p_E E^{(r)} + p_F F^{(r)} \}, \tag{2.18}$$

where the coefficients  $p_{CC}$ ,  $p_{CD}$ ,  $p_{DD}$ ,  $p_E$  and  $p_F$  are some polynomials in  $A^{(r)}$  and  $B^{(r)}$ . The above form for  $G(x, T)$  springs from the fact that all possible SAW paths, within the  $(r + 1)$ th-order fractal structure, can be made in five different ways, using the  $r$ th-order structures. The

structure of expression (2.18) shows that the asymptotic behaviour of  $G(x, T)$ , in the vicinity of the critical fugacity  $x_c(v)$ , depends on the corresponding behaviour of the restricted partition functions (2.2)–(2.7). Assuming that the singular behaviour of (2.18) is of the form (2.17), it can be shown that the critical exponent  $\gamma$  should be

$$\gamma = \frac{\ln \frac{6\lambda_\gamma^2}{b(b+1)(b+2)}}{\ln \lambda_\gamma}, \quad (2.19)$$

where  $\lambda_\gamma$  is the largest eigenvalue of the matrix formed of the coefficients  $c_1^* = c_1(A^*, B^*)$ ,  $c_2^* = c_2(A^*, B^*)$ ,  $d_1^* = d_1(A^*, B^*)$  and  $d_2^* = d_2(A^*, B^*)$  (that appear in the RG transformations (2.4) and (2.5)) evaluated at the non-trivial fixed points of the RG transformations (2.2) and (2.3), that is,

$$\lambda_\gamma = \frac{c_1^* + d_2^* + \sqrt{(c_1^* - d_2^*)^2 + 4d_1^*c_2^*}}{2}. \quad (2.20)$$

To verify forms (2.19) and (2.20), an intricate analysis, similar to those applied in [8], is necessary. Here we note that to learn specific values of  $\gamma$  in three different regions (that is to find exponents  $\gamma_E$ ,  $\gamma_\theta$  and  $\gamma_G$ ), for a set of the members of the 3D SG fractal family, one needs to calculate the two eigenvalues  $\lambda_v$  and  $\lambda_\gamma$ , at three different fixed points (2.9), (2.11) and (2.14), which correspond to the high temperature regions, to the vicinity of the  $\theta$ -point, and to the low temperature regions, respectively.

### 3. Presentation of the obtained results

We have calculated the critical exponent  $\gamma$ , associated with the total number of SAWs, and the critical exponent  $\phi_\theta$  which determines the average number  $\langle M \rangle$  of monomers being in contact, for a sequence of the 3D SG fractals. Before this work, only the value for the critical exponent  $\gamma$  was known in the high temperature region of the  $b = 2$  fractal [8]. Here we have calculated  $\gamma$  for  $2 \leq b \leq 40$ , and  $\phi_\theta$  for  $2 \leq b \leq 4$  by applying the exact and MCRG methods.

Exact calculation of  $\gamma$  requires knowledge of coefficients  $a(i, j)$  and  $b(i, j)$  that appear in (2.2) and (2.3) in order to find  $\lambda_v$  (which was done in [12] for  $2 \leq b \leq 4$ ). Besides, one should know coefficients of polynomials  $c_1$ ,  $c_2$ ,  $d_1$  and  $d_2$  (that appear in (2.4) and (2.5)) in order to find  $\lambda_\gamma$ . The latter can be calculated by enumerating the entire set of possible SAWs that are described by the restricted partition functions  $C^{(r)}$  and  $D^{(r)}$ . We have found that this enumeration is feasible in the cases  $b = 2, 3$  and  $4$ . More precisely, for  $b = 2$  the enumeration can be done straightforwardly [8], whereas for  $b = 3$  and  $b = 4$  it requires a reasonable computer facility (see the appendix).

For a sequence of  $b \geq 5$ , the exact determination of polynomials  $c_1$ ,  $c_2$ ,  $d_1$  and  $d_2$  cannot be accomplished using the present-day computers. However, one can surmount this problem because the calculation of  $\lambda_\gamma$  does not need a complete knowledge of polynomials  $c_1$ ,  $c_2$ ,  $d_1$  and  $d_2$  (that is, one does not need to know all their coefficients). In fact, for obtaining  $\lambda_\gamma$  one needs only values of the relevant polynomials at the appropriate fixed point (see equation (2.20)). Fortunately, the polynomials that appear in (2.4) and (2.5) can be conceived as the grand canonical partition functions of the appropriate ensembles and, consequently, within the MCRG method, the requisite values of polynomials can be accurately determined by numerical experiments. Details of the way to learn values of  $c_1^*$ ,  $c_2^*$ ,  $d_1^*$  and  $d_2^*$  are quite similar to the way applied previously [16, 17], and here we are not going to elaborate on it further.

In table 1 we present our exact and MCRG findings for  $\gamma_E$  for a sequence of the 3D SG fractals ( $2 \leq b \leq 40$ ). Before making an overall comparison of the exact and the MCRG results, it is interesting to observe that, for  $b = 2$  fractal, the value  $\gamma_E = 1.42 \pm 0.04$

**Table 1.** The exact ( $2 \leq b \leq 4$ ) and MCRG ( $2 \leq b \leq 40$ ) results for the critical exponents  $\gamma_E$  obtained in this work, in a high temperature region, described by the fixed points  $(A_E, B_E)$  [12], for the 3D SG family of fractals. The given error bars have been determined by statistics of the MC simulation. Each MCRG entry of the table has been obtained by performing  $5 \times 10^5$  MC simulations.

$b$	$(A_E, B_E)$	$\gamma_E$
2	(0.4294, 0.0499)	1.446 06
	(0.4311 $\pm$ 0.0009, 0.0505 $\pm$ 0.0023)	1.446 $\pm$ 0.017
3	(0.3419, 0.0239)	1.535 18
	(0.3421 $\pm$ 0.0004, 0.0245 $\pm$ 0.0015)	1.537 $\pm$ 0.011
4	(0.2899, 0.0122)	1.616 50
	(0.2898 $\pm$ 0.0004, 0.0122 $\pm$ 0.0020)	1.617 $\pm$ 0.010
5	(0.2560 $\pm$ 0.0004, 0.0067 $\pm$ 0.0019)	1.704 $\pm$ 0.011
6	(0.2319 $\pm$ 0.0003, 0.0038 $\pm$ 0.0012)	1.776 $\pm$ 0.012
7	(0.2148 $\pm$ 0.0003, 0.0020 $\pm$ 0.0018)	1.851 $\pm$ 0.013
8	(0.2016 $\pm$ 0.0003, 0.0012 $\pm$ 0.0026)	1.931 $\pm$ 0.014
9	(0.1912 $\pm$ 0.0004, 0.0007 $\pm$ 0.0008)	2.021 $\pm$ 0.015
10	(0.1829 $\pm$ 0.0003, 0.0005 $\pm$ 0.0023)	2.093 $\pm$ 0.016
12	(0.1703 $\pm$ 0.0004, 0.0001 $\pm$ 0.0035)	2.207 $\pm$ 0.019
15	(0.1581 $\pm$ 0.0001, -)	2.356 $\pm$ 0.025
17	(0.1525 $\pm$ 0.0001, -)	2.436 $\pm$ 0.030
20	(0.1464 $\pm$ 0.0001, -)	2.605 $\pm$ 0.041
25	(0.1399 $\pm$ 0.0001, -)	2.757 $\pm$ 0.059
30	(0.1355 $\pm$ 0.0001, -)	2.920 $\pm$ 0.076
35	(0.1327 $\pm$ 0.0001, -)	3.13 $\pm$ 0.16
40	(0.1306 $\pm$ 0.0001, -)	3.18 $\pm$ 0.28

was obtained by applying the series expansion method [18]. Comparing this value with the corresponding results (exact and MCRG) from table 1, it can be noticed that the MCRG result ( $1.446 \pm 0.017$ ) is definitely closer to the exact value (1.44606). Now we compare the results obtained, via the exact RG approach and through the MCRG technique, for the first three members ( $b = 2, 3, 4$ ) of the SG fractal family. One can observe that the MCRG results for the critical exponent  $\gamma_E$  deviate at most 0.8% from the exact results. This very good agreement provides confidence in applying the MCRG approach for a longer sequence of fractals ( $5 \leq b \leq 40$ ). For the sake of a better assessment of the global behaviour of the critical exponent  $\gamma_E$  as a function of the fractal scaling parameter  $b$ , we depict the corresponding values (from table 1) in figure 3. One can see that  $\gamma_E$ , being always larger than recently obtained three-dimensional Euclidean values ( $\gamma_E(d = 3) = 1.1585$  [3],  $\gamma_E(d = 3) = 1.1581 \pm 0.0025 \pm 0.0033$  [6],  $\gamma_E(d = 3) = 1.1575 \pm 0.0006$  [7]), monotonically increases with  $b$  (in the studied interval,  $2 \leq b \leq 40$ ). Here one encounters the provocative question about the behaviour of  $\gamma_E$  for large  $b$ , and in particular for  $b \rightarrow \infty$ . To answer this question one may try to adopt the finite-size scaling method which was successfully applied [19] in the case of the 2D SG family of fractals (with the prediction that  $\gamma_E$  for very large  $b$  goes, from below, to the non-Euclidean value, that is, it goes to  $133/32$  instead of  $43/32$ ). Finally, it is interesting to compare obtained values of  $\gamma_E$  with other results found for the 3D fractals. However, we have been able to locate only the work [20] in which the exponent  $\gamma_E$  for SAWs on the 3D Sierpinski carpet fractal, labelled by  $(n, k) = (3, 7)$ , was calculated. For this fractal (whose fractal dimension is equal to  $d_f = 2.727$ ) the value  $\gamma_E = 1.36 \pm 0.03$  was numerically predicted. One may observe that the latter value is larger than the 3D Euclidean value ( $\gamma_E \approx 1.158$ ), and besides it appears to be smaller than all known values of  $\gamma_E$  (see table 1) for the 3D SG fractals.



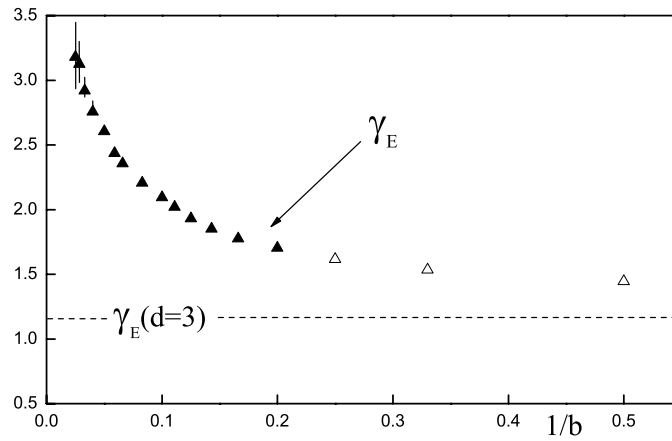


**Figure 3.** The exact (open triangles) and the MCRG (solid triangles) results for the extended phase critical exponent  $\gamma_E$  as a functions of the scale parameter  $b$ . The Euclidean value for  $\gamma_E(d=3) \approx 1.158$ , that springs from three different approximate numerical findings [3, 6, 7], is represented by the dashed horizontal line. The error bars, for the MCRG results, are smaller than the height of the corresponding symbols (solid triangles) for all  $b \leq 20$ .

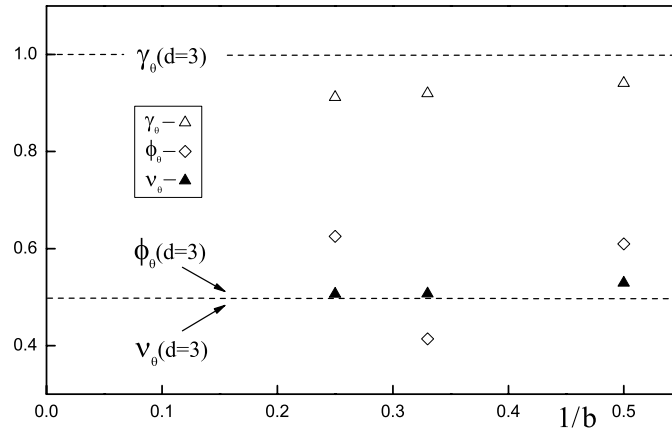


**Figure 4.** The exact results for the critical exponents  $\gamma_\theta$  (open triangles),  $\phi_\theta$  (open diamonds), and  $\nu_\theta$  (solid triangles) as a functions of the scale parameter  $b$ . The corresponding Euclidean values  $\gamma_\theta(d=3) = 1$ ,  $\phi_\theta(d=3) = 1/2$  and  $\nu_\theta(d=3) = 1/2$  are depicted by dashed horizontal lines.

**Table 2.** Values of the critical exponents  $\phi_\theta$ ,  $\gamma_\theta$  and  $\gamma_G$  obtained in this work, via exact renormalization group approach, for two different phases ( $\theta$ -chain and collapsed SAW) on 3D SG fractals. For the sake of completeness, we quote here the values for the fixed points  $((A_\theta, B_\theta)$  and  $(A_G, B_G)$ ) and critical exponents ( $\nu_\theta$  and  $\nu_G$ ) for  $b = 2$ ,  $b = 3$  and  $b = 4$  fractals, that was obtained in [9], [10] and [12] respectively.

$b$	$A_\theta$	$B_\theta$	$\nu_\theta$	$\phi_\theta$	$\gamma_\theta$	$A_G$	$B_G$	$\nu_G$	$\gamma_G$
2	1/3	1/3	0.5294	0.60986	0.94119	0	$22^{-1/3}$	1/2	-1
3	0.2071	0.4307	0.5072	0.41374	0.91994	0	$\infty$	0.4819	-
4	0.1929	0.3388	0.5067	0.62545	0.91219	0	$22^{-1/3}$	1/2	-1.0805

In figure 4 we present our exact findings for the critical exponents  $\phi_\theta$ ,  $\gamma_\theta$  and  $\nu_\theta$ , which correspond to the polymer  $\theta$ -point behaviour (see, also, results presented in table 2). First, we

can see that all obtained exact values of  $\gamma_\theta$ , which monotonically decrease with increase of the scaling parameter  $b$ , are less than the three-dimensional Euclidean mean field prediction  $\gamma_\theta = 1$  (which was confirmed by the numerical result  $\gamma_\theta(d = 3) = 0.9985 \pm 0.0035 \pm 0.0033$  of Monte Carlo simulations performed on 3D Euclidean lattice [6]). Next, we may observe that the behaviour of the critical exponent  $\phi_\theta$ , within the available region of  $b$ , is at present inconclusive. Eventually, concerning the behaviour of the critical exponent  $\nu_\theta$ , the exact results presented in figure 4 show that  $\nu_\theta$ , being always larger than the 3D Euclidean value  $1/2$ , monotonically decrease with increase of  $b$ . At this point we again meet the situation when we cannot say anything about the asymptotic behaviour of studied critical exponents at the  $\theta$ -point. Specifically, it is challenging to deduce whether  $\nu_\theta$  becomes smaller than the Euclidean value  $1/2$  (what, in fact, happens in the high temperature region [12]). To answer this question by applying the MCRG method appears to be forbiddingly difficult task, because of the instability of the corresponding  $\theta$  fixed points. This challenge is more interesting in the light of the fact that was found [2] (through the  $\epsilon = 3 - d$  expansion) that in the 3D Euclidean case all critical exponents  $\phi_\theta$ ,  $\gamma_\theta$ , and  $\nu_\theta$  approach the mean field predictions via larger values.

Finally, we may comment on the obtained values for the critical exponent  $\gamma_G$  (see table 2). The given values are obtained in accord with formula (2.15) that was assumed to be valid for all temperature regions. However, at low temperatures it was argued [21] that adequate formula should be

$$C_N \sim \mu_0^N \mu_1^{N^\sigma} N^{\gamma_G - 1}, \quad (3.1)$$

where  $\mu_0(T)$  and  $\mu_1(T)$  are respectively bulk and perimeter monomer fugacities, both depending on the temperature  $T$ . In the 3D Euclidean case  $\sigma = 2/3$ . So far, there has not been much work concerning the correct value of  $\gamma_G$ , and accordingly this problem remains unravelled.

#### 4. Summary

In this paper, we have studied self-interacting self-avoiding walk (SAW) situated on fractal structures represented by the three-dimensional (3D) Sierpinski gasket (SG) family of fractals. Specifically, we have calculated the critical exponents  $\gamma$  (associated with the total number of distinct SAWs) in the three different phases (extended,  $\theta$ -point and globular) that occur in the case when the interactions between non-consecutive adjacent monomers are present. It should be pointed out that this exponent has not been calculated in previous attacks of the described problem.

By applying the exact renormalization group method (for  $b = 2, 3$  and  $4$ ) we have calculated specific results for the critical exponents  $\gamma_E$ ,  $\gamma_\theta$  and  $\gamma_G$ , for the three different phases. In addition, we obtained the crossover critical exponent  $\phi_\theta$  associated with the average number of monomers in contact at the  $\theta$ -point. The specific accomplishment in the course of this work is the calculation of a long sequence of values of  $\gamma_E$ , for  $2 \leq b \leq 40$ , obtained by applying the Monte Carlo renormalization group method. Our results demonstrate that the critical exponent  $\gamma_E$ , for the studied values of  $b$ , being always larger than the corresponding three-dimensional Euclidean value  $\gamma_E \approx 1.158$ , monotonically increases with  $b$ . On the other hand,  $\gamma_\theta$  (for  $b = 2, 3$  and  $4$ ), being always smaller than the corresponding Euclidean value ( $\gamma_\theta = 1$ ), seems to monotonically decrease with  $b$ , whereas the crossover critical exponent  $\phi_\theta$  (for the same values of  $b$ ) does not display a definite trend.

On the exposed grounds of the presented investigation we may conclude that the set of obtained results of the studied problem (the case of self-interacting SAWs on the 3D fractals) has been significantly extended. As a further investigation one may try to extend our results

by some other method, for instance by applying the finite-size scaling technique. Thereby our findings contribute to the endeavour to achieve an insight of the same problem on the 3D Euclidean lattice.

### Acknowledgments

This paper has been done as a part of the work within the project no 1634 funded by the Serbian Ministry of Science and Protection of the Life Environment.

### Appendix

In this appendix, we give the exact shape of the polynomials  $c_1$ ,  $c_2$ ,  $d_1$  and  $d_2$  that appears in RG equations (2.4) and (2.5). We have found that these polynomials have the following form:

$$c_1(A, B) = \sum_{i,j} C_1(i, j) A^i B^j, \quad (\text{A.1})$$

$$c_2(A, B) = \sum_{i,j} C_2(i, j) A^i B^j \quad (\text{A.2})$$

$$d_1(A, B) = \sum_{i,j} D_1(i, j) A^i B^j, \quad (\text{A.3})$$

$$d_2(A, B) = \sum_{i,j} D_2(i, j) A^i B^j, \quad (\text{A.4})$$

where, in the case  $b = 2$ , the nonzero values of coefficients  $C_1(i, j)$ ,  $C_2(i, j)$ ,  $D_1(i, j)$  and  $D_2(i, j)$  are

$$\begin{aligned} C_1(0, 0) &= 1, C_1(1, 0) = 3, C_1(2, 0) = 6, C_1(2, 1) = 6, C_1(3, 0) = 6, \\ C_2(2, 0) &= 6, C_2(2, 1) = 18, C_2(3, 0) = 12, \\ D_1(2, 0) &= 1, D_1(2, 1) = 3, D_1(3, 0) = 2, \\ D_2(0, 3) &= 22, D_2(1, 2) = 22, D_2(2, 0) = 3, D_2(2, 1) = 16, D_2(3, 0) = 7 \end{aligned}$$

whereas for  $b = 3$  they are,

$$\begin{aligned} C_1(0, 0) &= 1, C_1(1, 0) = 3, C_1(2, 0) = 15, C_1(2, 1) = 6, C_1(2, 2) = 18, C_1(3, 0) = 48, \\ C_1(3, 1) &= 54, C_1(3, 2) = 96, C_1(3, 3) = 72, C_1(3, 4) = 132, \\ C_1(3, 5) &= 240, C_1(4, 0) = 132, \\ C_1(4, 1) &= 210, C_1(4, 2) = 444, C_1(4, 3) = 1104, C_1(4, 4) = 1836, C_1(5, 0) = 312, \\ C_1(5, 1) &= 750, C_1(5, 2) = 1368, C_1(5, 3) = 2268, C_1(5, 4) = 2976, C_1(6, 0) = 576, \\ C_1(6, 1) &= 1596, C_1(6, 2) = 2958, C_1(6, 3) = 3588, C_1(7, 0) = 792, \\ C_1(7, 1) &= 2154, C_2(7, 2) = 2748, C_1(8, 0) = 780, C_1(8, 1) = 1722, C_1(9, 0) = 378, \\ C_2(2, 0) &= 6, C_2(2, 1) = 18, C_2(3, 0) = 30, C_2(3, 1) = 78, C_2(3, 2) = 72, C_4(3, 3) = 132, \\ C_2(3, 4) &= 240, C_2(3, 5) = 960, C_2(4, 0) = 102, C_2(4, 1) = 252, C_2(4, 2) = 1044, \\ C_2(4, 3) &= 3432, C_2(4, 4) = 5088, C_2(5, 0) = 372, C_2(5, 1) = 1290, C_2(5, 2) = 3060, \\ C_2(5, 3) &= 6492, C_2(5, 4) = 9576, C_2(6, 0) = 888, C_2(6, 1) = 3390, C_2(6, 2) = 8796, \\ C_2(6, 3) &= 15\,144, C_2(7, 0) = 1368, C_2(7, 1) = 4848, C_2(7, 2) = 8964, C_2(8, 0) = 1668, \end{aligned}$$

$$\begin{aligned}
C_2(8, 1) &= 5256, C_2(9, 0) = 1050, \\
D_1(2, 4) &= 66, D_1(2, 7) = 1304, D_1(3, 0) = 1, D_1(3, 2) = 12, D_1(3, 3) = 44, \\
D_1(3, 4) &= 244, D_1(3, 5) = 1400, D_1(3, 6) = 2420, D_1(4, 0) = 9, D_1(4, 1) = 23, \\
D_1(4, 2) &= 62, D_1(4, 3) = 410, D_1(4, 4) = 1428, D_1(4, 5) = 4632, D_1(5, 0) = 40, \\
D_1(5, 1) &= 149, D_1(5, 2) = 474, D_1(5, 3) = 1632, D_1(5, 4) = 3126, D_1(6, 0) = 115, \\
D_1(6, 1) &= 507, D_1(6, 2) = 1456, D_1(6, 3) = 2912, D_1(7, 0) = 241, D_1(7, 1) = 983, \\
D_1(7, 2) &= 1962, D_1(8, 0) = 303, D_1(8, 1) = 798, D_1(9, 0) = 202, \\
D_2(2, 3) &= 66, D_2(2, 6) = 1304, D_2(2, 7) = 4308, D_2(3, 2) = 66, D_2(3, 3) = 134, \\
D_2(3, 4) &= 1400, D_2(3, 5) = 7068, D_2(3, 6) = 27088, D_2(4, 0) = 9, D_2(4, 1) = 64, \\
D_2(4, 2) &= 296, D_2(4, 3) = 1900, D_2(4, 4) = 8448, D_2(4, 5) = 23684, D_2(5, 0) = 72, \\
D_2(5, 1) &= 354, D_2(5, 2) = 2062, D_2(5, 3) = 8442, D_2(5, 4) = 24064, D_2(6, 0) = 224, \\
D_2(6, 1) &= 1512, D_2(6, 2) = 5870, D_2(6, 3) = 15172, D_2(7, 0) = 566, D_2(7, 1) = 3310, \\
D_2(7, 2) &= 8696, D_2(8, 0) = 793, D_2(8, 1) = 2854, D_2(9, 0) = 620.
\end{aligned}$$

For  $b = 4$  the pertinent coefficients require much more space (four printed pages) and we do not give them here (the relevant data are, however, available upon request addressed to the authors).

## References

- [1] Vanderzande C 1998 *Lattice Models of Polymers* (Cambridge: Cambridge University Press)
- [2] Duplantier B 1987 *J. Chem. Phys.* **86** 4233
- [3] MacDonald D, Joseph S, Hunter D L, Moseley N J, Jan N and Guttmann A J 2000 *J. Phys. A: Math. Gen.* **33** 5973
- [4] Grassberger P 1993 *J. Phys. A: Math. Gen.* **26** 2769
- [5] Grassberger P and Hegger R 1995 *J. Chem. Phys.* **102** 6881
- [6] Nidras P P 1996 *J. Phys. A: Math. Gen.* **29** 7929
- [7] Caracciolo S, Causo M S and Pelissetto A 1998 *Phys. Rev. E* **57** R1215
- [8] Dhar D 1978 *J. Math. Phys.* **19** 5
- [9] Dhar D and Vannimenus J 1987 *J. Phys. A: Math. Gen.* **20** 199
- [10] Knežević M and Vannimenus J 1987 *J. Phys. A: Math. Gen.* **20** L969
- [11] Maričić J and Elezović-Hadžić S 2002 *Preprint cond-mat/0205509*
- [12] Elezović-Hadžić S, Živić I and Milošević S 2003 *J. Phys. A: Math. Gen.* **36** 1213
- [13] Kumar S, Singh Y and Joshi Y P 1990 *J. Phys. A: Math. Gen.* **23** 2987
- [14] Prellberg T and Owczarek A L 1995 *Phys. Rev. E* **51** 2142
- [15] Brak R, Owczarek A L and Prellberg T 1993 *J. Phys. A: Math. Gen.* **26** 4565
- [16] Živić I and Milošević S 1993 *J. Phys. A: Math. Gen.* **26** 3393
- [17] Milošević S and Živić I 1994 *J. Phys. A: Math. Gen.* **27** 7739
- [18] Ordemann A, Porto M and Roman H E 2002 *Phys. Rev. E* **65** 021107
- [19] Dhar D 1988 *J. Phys.* **49** 397
- [20] Ordemann A, Porto M and Roman H E 2002 *J. Phys. A: Math. Gen.* **35** 8029
- [21] Owczarek A L, Prellberg T and Brak R 1993 *Phys. Rev. Lett.* **70** 951